

# Holographic QCD with Isospin Chemical Potential

Andrei Parnachev

*C.N.Yang Institute for Theoretical Physics, SUNY, Stony Brook, NY 11794-3840, USA*

## Abstract

We consider configurations of  $D4 - D8 - \overline{D}8$  branes which correspond to large  $N$  QCD with non-vanishing temperature and chemical potential for baryon number and isospin. We study the holographic dual of this model and find a rich phase structure. The phases, distinguished by the values of quark condensates, are separated by the surfaces of first order phase transitions. The picture is in many respects similar to the expected phase structure of QCD in the chiral limit.

## 1. Introduction and summary

String theoretic constructions aimed at describing the theory of strong interactions, QCD, are becoming more and more elaborate. There are now many versions of the gauge/string correspondence where many constraints of the  $\mathcal{N} = 4$  Super Yang Mills are relaxed, although one still has to consider the limit of large number of colors  $N$ . However the description of large  $N$  QCD-like (asymptotically free) theories proves to be a hard task. Typically, the regime where the gauge theory is modified at energies much higher than the dynamically generated scale, is not easily tractable on the dual, string theoretic side.

Despite these limitations, holographic models are still useful because very often they capture physics qualitatively correct. Hence, they provide a unique window into the dynamics of strongly coupled gauge theories. With more luck, it might be possible to extract quantities that are universal, i.e. do not significantly change as one interpolates between the holographic dual and QCD. A good place to search for such universal quantities is the phase diagram of the theory, especially if the second order phase transitions are present.

A model proposed in [1] building on [2] which involves a certain configuration of  $D4 - D8 - \overline{D8}$  branes is particularly interesting because it gives rise to large  $N$  QCD with quarks in a certain region of the parameter space. This model, also sometimes called “holographic QCD”, has a holographic dual which reproduces some expected physics of the gauge theory. Chiral symmetry breaking and derivation of the pion lagrangian have been described in the original paper by Sakai and Sugimoto [1]. The model has been also investigated at finite temperature [3,4]. Nonzero baryon chemical potential has been considered in [5,6] where the phase diagram was shown to contain a line of first order phase transitions in the  $\mu_B - T$  plane.<sup>1</sup>

In this paper we focus our attention on the case of two flavor ( $N_f = 2$ ) large  $N$  holographic QCD with non-vanishing isospin chemical potential, whose value we denote by  $\mu_I$ . QCD with  $\mu_I \neq 0$  has been studied in the variety of models (see [13-16] for an incomplete list of references.) The phase diagram enjoys rich structure, with first and second order phase transition lines separating various phases. This therefore is a promising

---

<sup>1</sup> In the first versions of [5] the solution with broken chiral symmetry contained an unphysical charge. This has been corrected in [6] and in the most recent version of [5]. Recent work which discusses related physics and possible additional phases includes [7-11]. The isospin chemical potential in the  $D3 - D7$  system was recently discussed in [12].

setting for the search of universal quantities. Besides, theory with non-vanishing  $\mu_I$  is amenable to lattice simulations and does not suffer from the determinant sign problem, which complicates obtaining lattice results for the  $\mu_B \neq 0$  case. Finally, non-vanishing isospin chemical potential can be experimentally relevant.

The holographic dual of the  $D4 - D8 - \overline{D8}$  branes involves the warped product of four-dimensional Minkowski space, a circle parameterized by  $X^4 \in [0, 2\pi R_4)$ , a holographic coordinate  $U > U_K$  and a four-sphere (more details are provided below). At non-zero temperature the phase where gluons are not confined is described by a black hole metric which is thermodynamically preferred for temperatures higher than  $1/2\pi R_4$ . Most of the analysis below will be restricted to this phase. We comment on the appearance of confinement/deconfinement transition in the phase diagram in Section 4.

Fundamental matter is described by  $N_f$  pairs of  $D8 - \overline{D8}$  branes with asymptotic separation  $L$ . The low energy degrees of freedom which live on the intersections of the  $D8$  and  $\overline{D8}$  branes with the  $D4$  branes are four-dimensional massless left and right-handed quarks. This brane setup thus describes large  $N$  QCD in the chiral limit (in the certain region of the parameter space). At generic values of baryon and isospin chemical potentials, the  $D8$  branes exist in two phases. In the curved phase  $D8$  and  $\overline{D8}$  branes connect and hence chiral symmetry is broken. In the straight phase, the flavor branes are located at constant values of  $X^4$  and fall into the horizon of the black hole. This phase of restored chiral symmetry is preferred at larger values of  $T$  and  $\mu_B$ .

The phase diagram of the system depends on dimensionless parameters  $LT$  and  $\tilde{\mu}_i = \mu_i/E_0$  where  $E_0 = 4\pi\lambda/L^2$  sets the scale of chemical potential. ( $\lambda$  is the t'Hooft coupling of five-dimensional gauge theory on the  $D4$  branes, which becomes four-dimensional after Kaluza-Klein reduction.) Fig. 1 contains the picture of the phase diagram in the limit  $LT \rightarrow 0$ . (It is instructive to compare it with Fig. 1 in [14].) The fundamental domain can be taken to be

$$-\tilde{\mu}_1 \leq \tilde{\mu}_2 \leq \tilde{\mu}_1; \quad \tilde{\mu}_1 \geq 0 \quad (1.1)$$

The phases are distinguished by the values of the condensates:

$$\sigma_i = \langle \overline{\psi}_i \psi_i \rangle, \quad i = 1, 2; \quad \rho = \langle \overline{\psi}_i \gamma^5 \tau_{ij}^2 \psi_j \rangle \quad (1.2)$$

where  $\tau^3$  is the Pauli matrix in the flavor space. In the upper right triangle defined by  $\tilde{\mu}_1, \tilde{\mu}_2 \geq \tilde{\mu}_c = 0.11$  all condensates vanish. Curved blue line separates the phase with non-zero pion condensate  $\rho$  at small  $\mu_B$  (below the line) from the phases with  $\sigma_1 \neq 0, \sigma_2 = 0$

for  $-\tilde{\mu}_c \leq \tilde{\mu}_2 \leq \tilde{\mu}_c$  and  $\sigma_{1,2} = 0$  for  $\tilde{\mu}_2 \leq \tilde{\mu}_c$ . All these features are also present in Fig. 1 of ref. [14]. What is not present in our analysis is the second order phase transition of [14] which separates the phase with  $\rho \neq 0$  at small  $\tilde{\mu}_I$  from the phase with  $\sigma_{1,2}, \rho = 0$  at larger  $\tilde{\mu}_I$ . This line might be an artifact of the random matrix model used in [14].<sup>2</sup>

So far we discussed the  $LT \rightarrow 0$  case. The diagram does not qualitatively change as we increase  $LT$  (see Figs. 5,6), although the value of  $\tilde{\mu}_c$  decreases until it reaches zero at  $LT \approx 0.15$  (Fig. 4). This corresponds to the temperature of chiral phase transition at  $\mu_B = 0$ . The full phase diagram should be drawn in three dimensions, with Figs. 1,2,5,6 representing slices at two different values of  $LT$ . The surface of the first order phase transitions which is represented by the blue curves on the pictures of these slices looks in fact somewhat similar to a hyperboloid, with  $\mu_I$  axis being the axis of rotation. (Of course, there is no rotational symmetry in the  $\mu_B - T$  plane in our case)

The rest of the paper is organized as follows. In the next section we set up the notation, and discuss general expectations. We then consider  $LT \rightarrow 0$  case, establish the necessary holographic dictionary and present some analytic and numerical results. In Section 3 we consider finite temperature case, where most of the analysis is numerical. Here we sketch the form of the three-dimensional phase diagram. We conclude in Section 4.

## 2. Nonzero chemical potentials; small temperature

We consider  $SU(N)$  gauge theory with  $N_f = 2$  massless quarks (each described by a single Dirac spinor  $\psi_i$ ,  $i = 1, 2$ ) in the large  $N$  limit. Various phases of the theory can be distinguished by the values of the condensates (1.2). The matter part of the Lagrangian is

$$\mathcal{L}_q = \sum_{i=1,2} \bar{\psi}_i [\gamma^\mu (\partial_\mu + iA_\mu) + \mu_i \gamma^0] \psi_i \quad (2.1)$$

where sum over color indexes of  $SU(N)$  is implied. Baryon and isospin chemical potential are defined to be

$$\mu_B = \frac{1}{2}(\mu_1 + \mu_2); \quad \mu_I = \frac{1}{2}(\mu_1 - \mu_2) \quad (2.2)$$

respectively. At  $\mu_{1,2} = 0$  the Lagrangian has  $SU(2) \times SU(2)$  global symmetry. One can use the axial part of this symmetry to rotate the  $\sigma_{1,2}$  condensates into  $\rho$ ; these condensates

---

<sup>2</sup> In the view of our motivation, the absence of the second order phase transition is a slight disappointment.

develop nonzero expectation values, and spontaneously break chiral symmetry. The corresponding Nambu-Goldstone model is the pion. At non-zero value of  $\mu_I$  (and sufficiently small  $\mu_{1,2}$ ) the system is supposed to prefer nonzero value for  $\rho$  together with  $\sigma_{1,2} = 0$ . (see e.g. [14].)

This large  $N$  QCD has a holographic dual, which is obtained by going to the near-horizon geometry of the  $D4$  branes on a circle of radius  $R_4$  [2] and adding  $N_f = 2$   $D8 - \overline{D8}$  pairs [1]. The model deviates from QCD at energy scales  $\sim 1/R_4$  which is related to the dynamically generated scale as

$$\Lambda_{QCD} \sim \frac{1}{R_4} e^{-\frac{1}{\lambda_4}} \quad (2.3)$$

where  $\lambda_4 = \lambda/R_4$  is the four-dimensional t'Hooft coupling at the cutoff scale. As customary in the holographic models, when the scales are widely separated,  $\lambda_4$  is small, which corresponds to the strong curvature regime in string theory. This is beyond the reach of the present string-theoretic technology. We consider instead the opposite regime of large  $\lambda_4$  where string theory reduces to supergravity + low energy  $D8$ -brane dynamics.

In this Section we restrict to the regime of small temperatures,  $LT \rightarrow 0$ . We assume that confinement energy scale is much smaller than the scale associated with the dynamics of fundamental matter ( $1/R_4 \ll 1/L$ ), and even at these small temperature glue is deconfined.<sup>3</sup> (It is not hard to reinstate the effects of confinement/deconfinement transition on the phase diagram - we do it in Section 4. )

The euclidean metric of the holographic dual is given by

$$ds^2 = \left(\frac{U}{R}\right)^{\frac{3}{2}} (\eta_{\mu\nu} dX^\mu dX^\nu + (dX^4)^2) + \left(\frac{U}{R}\right)^{-\frac{3}{2}} [(dU)^2 + U^2 d\Omega_4^2] \quad (2.4)$$

There is also non-trivial dilaton

$$e^\Phi = g_s \left(\frac{U}{R}\right)^{\frac{3}{4}} \quad (2.5)$$

The length scale  $R$  is related to the parameters of the gauge theory as

$$R^3 = \pi\lambda = \pi g_s N \quad (2.6)$$

Here and in the rest of the paper the string length  $l_s = 1$ . The dynamics of the fundamental matter is described by the DBI action of  $N_f = 2$   $D8 - \overline{D8}$  pairs. Asymptotically (as  $U \rightarrow \infty$ ) the branes and antibranes are separated by coordinate distance  $L$  in the  $X^4$  direction.

---

<sup>3</sup> Formally, this limit is equivalent to the NJL limit studied in [17-19]

They may connect at smaller values of  $U$ . This configuration spontaneously breaks chiral symmetry. Gauge fields on the  $D8$  branes are holographically dual to the currents of global  $SU(2) \times SU(2)$  symmetry. As in [6] it is convenient to go to the gauge  $A_U = 0$  and Wick rotate  $A_0 \rightarrow iA_0$ . Then, the non-zero chemical potential in the lagrangian (2.1) corresponds to non-trivial boundary conditions on the values of  $A_0$ :

$$A_{0i}(U \rightarrow \infty) = \mu_i; \quad i = 1, 2 \quad (2.7)$$

where  $A_{0i}$  is the abelian part of the field on the  $i$ -th brane and antibrane.

In the absence of external charges, baryon chemical potential cannot affect the curved solution [6]. Hence, for the purpose of computing the action, we can set  $\mu_1 = -\mu_2 = \mu_I$  in this phase. There are now two possible curved brane solutions. One solution involves the brane with  $A_0(U \rightarrow \infty) = \pm\mu$  connecting with the antibrane with  $A_0(U \rightarrow \infty) = \pm\mu$ . This solution has zero electric field on the resulting curved flavor branes and non-zero condensates  $\sigma_1 = \sigma_2$ . As explained in [17] the holographic dual of the chiral condensate involves a non-trivial profile of the open string tachyon and hence is difficult to analyze in the DBI approximation.

Another solution involves brane with  $A_0(U \rightarrow \infty) = \pm\mu$  connecting with the antibrane with  $A_0(U \rightarrow \infty) = \mp\mu$ . There is nonzero electric field of opposite direction, but same magnitude on two curved branes so the branes overlap again. This solution is obtained from the previous one by chiral rotation, and hence corresponds to nonzero value of  $\rho$ .

In the following we will use the fact that in the connected phase  $(\partial_U A_{01})^2 = (\partial_U A_{02})^2$  and  $X_1^4 = X_2^4$  where the subscript corresponds to the isospin. The DBI action, up to an overall constant, is given by

$$S = 2 \int dU U^{\frac{5}{2}} \sqrt{1 - (\partial_U A_0)^2 + \left(\frac{U}{R}\right)^3 (\partial_U X^4)^2} \quad (2.8)$$

where a factor of two in front of the action counts the number of flavors and is added for convenience. (Since the only non-vanishing component of the gauge field is  $A_0(U)$ , the Chern-Simons term vanishes.) Lagrange-Euler equation of motion for the gauge field on the branes implies the existence of the conserved quantity,

$$\frac{U^{\frac{5}{2}} (\partial_U A_0)}{\sqrt{1 - (\partial_U A_0)^2 + \left(\frac{U}{R}\right)^3 (\partial_U X^4)^2}} = c \quad (2.9)$$

Eq. (2.9) can also be written as

$$(\partial_U A_0)^2 = c^2 \frac{1 + \left(\frac{U}{R}\right)^3 (\partial_U X^4)^2}{U^5 + c^2} \quad (2.10)$$

Likewise, the equation of motion for  $X^4$  can be written as

$$(\partial_U X^4)^2 = \frac{U_0^3 (U_0^5 + c^2) R^3}{U^6 (U^5 + c^2) - U_0^3 (U_0^5 + c^2) U^3} \quad (2.11)$$

where  $U_0$  labels the turning point: it is the value of the  $U$  coordinate where  $\partial_U X^4 \rightarrow \infty$ . To obtain (2.11) we expressed  $(\partial_U X^4)$  in terms of the constants of the equations of motion and then demanded  $\partial_U X^4 \rightarrow \infty$  at  $U = U_0$ . Substituting (2.11) back into (2.10) gives

$$(\partial_U A_0)^2 = \frac{c^2 U^3}{U^3 (U^5 + U_0^5 \tilde{c}^2) - U_0^8 (1 + \tilde{c}^2)} \quad (2.12)$$

where we introduced  $\tilde{c}$  via  $c^2 = U_0^5 \tilde{c}^2$ . Let us consider the phase with  $\partial_U A_1 = -\partial_U A_2$ . We need to re-express the values of the integrals of motion through  $\mu_{1,2}$  and  $L$ . Starting with the former, we have

$$\frac{1}{2} |\mu_1 - \mu_2| = \int_{U_0}^{\infty} dU |\partial_U A_0| = U_0 F(\tilde{c}) \quad (2.13)$$

where we used (2.12) in the second equality. We also pass to the rescaled quantities and define  $F(\tilde{c})$  as

$$F(\tilde{c}) = \int_1^{\infty} dx \sqrt{\frac{x^3 \tilde{c}^2}{x^3 (x^5 + \tilde{c}^2) - (1 + \tilde{c}^2)}} \quad (2.14)$$

Note that  $F(\tilde{c})$  is a monotonic function which satisfies  $F(0) = 0$  and

$$F(\tilde{c}) \sim \tilde{c} + o(\tilde{c}), \quad \tilde{c} \ll 1 \quad (2.15)$$

In the opposite regime of large  $\tilde{c}$

$$F(\tilde{c}) \approx c_1 \tilde{c}^{\frac{2}{5}}, \quad c_1 = \int_0^{\infty} \frac{dx}{\sqrt{1+x^5}} = \frac{\Gamma\left(\frac{3}{10}\right) \Gamma\left(\frac{6}{5}\right)}{\sqrt{\pi}} \quad (2.16)$$

Similarly, the separation of the branes can be computed as

$$\frac{L}{2} = \int_{U_0}^{\infty} dU \partial_U X^4 = \sqrt{\frac{\pi \lambda}{U_0}} G(\tilde{c}) \quad (2.17)$$

where

$$G(\tilde{c}) = \int_1^{\infty} dx \sqrt{\frac{1 + \tilde{c}^2}{x^6 (x^5 + \tilde{c}^2) - x^3 (1 + \tilde{c}^2)}} \quad (2.18)$$

which is a monotonically increasing function with

$$G(0) = \frac{2\sqrt{\pi}\Gamma\left(\frac{9}{16}\right)}{\Gamma\left(\frac{1}{16}\right)}, \quad \lim_{\tilde{c} \rightarrow \infty} G(\tilde{c}) = \frac{2\sqrt{\pi}\Gamma\left(\frac{2}{3}\right)}{\Gamma\left(\frac{1}{6}\right)} \quad (2.19)$$

We can use (2.17) to re-express

$$U_0 = E_0 G^2(\tilde{c}), \quad E_0 = \frac{4\pi\lambda}{L^2} \quad (2.20)$$

and then substitute the result into eq. (2.13)

$$\frac{1}{2}|\tilde{\mu}_1 - \tilde{\mu}_2| = F(\tilde{c})G^2(\tilde{c}) \quad (2.21)$$

where  $\tilde{\mu} \equiv \mu/E_0$ . Eq. (2.21) determines the value of  $\tilde{c}$  in terms of  $\tilde{\mu}$ . Next we need to compute the action. To regularize, we subtract the value of the action from that of a pair of straight branes ( $\partial_U X^4 = 0$ ) with vanishing chemical potential.<sup>4</sup> The resulting quantity is

$$\delta S = 2 \left[ \int_0^{U_0} dU U^{\frac{5}{2}} + \int_{U_0}^{\infty} \left( U^{\frac{5}{2}} - U^{\frac{5}{2}} \sqrt{1 - (\partial_U A_0)^2 + \left(\frac{U}{R}\right)^3 (\partial_U x^4)^2} \right) \right] \quad (2.22)$$

With the help of (2.20) this can also be written as

$$\delta S = 2E_0^{\frac{7}{2}} G^7(\tilde{c}) H(\tilde{c}) \quad (2.23)$$

where

$$H(\tilde{c}) = \frac{2}{7} + \int_1^{\infty} x^{\frac{5}{2}} \left( 1 - \sqrt{\frac{x^8}{x^3(x^5 + \tilde{c}^2) - (1 + \tilde{c}^2)}} \right) \quad (2.24)$$

This should be compared with the action for the phase where the branes are curved but have zero electric field. (This is the phase with  $\sigma_{1,2} \neq 0, \rho = 0$ .)

$$\delta S_0 = 2E_0^{\frac{7}{2}} G^7(0) H(0) \quad (2.25)$$

The thermodynamically preferred phase has a larger value of  $\delta S$ . One can check that (2.23) is larger or equal to (2.25), and hence as soon as  $\mu_I \neq 0$  the phase with  $\rho \neq 0$  is

---

<sup>4</sup> Another popular regularization scheme involves introducing an ultraviolet (large  $U$ ) cut-off for the integral. Since we are interested in the difference between the actions for different configurations, these regularizations are equivalent.



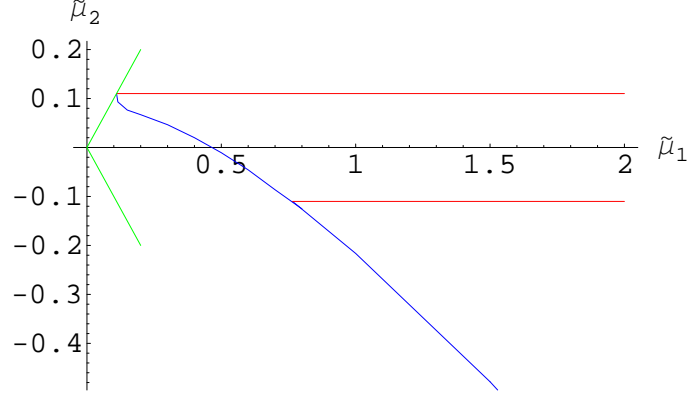


**Fig 1.** Phase diagram for  $LT \rightarrow 0$ .  $\mu_{1,2}$  are horizontal and vertical axes. Green lines  $\tilde{\mu}_2 = \pm\tilde{\mu}_1$  are boundaries of the fundamental domain. Solid blue and red curves are the lines of first order phase transitions. The phase between the red lines has  $\sigma_2 \neq 0$ . The phase between the blue and the green lines has  $\rho \neq 0$ . All other condensates vanish.

thermodynamically preferred. An interesting limit of (2.24) is  $\tilde{c} \rightarrow \infty$ , which corresponds to the large values of  $\tilde{\mu}_I$ ,

$$H(\tilde{c}) \approx \frac{2c_1}{7} \tilde{c}^{\frac{7}{5}} \quad (2.26)$$

which corresponds to

$$\delta S \approx \frac{2E_0^{\frac{7}{2}}}{7c_1^{\frac{5}{2}}} \frac{|\tilde{\mu}_1 - \tilde{\mu}_2|^{\frac{7}{2}}}{2^{\frac{5}{2}}} \quad (2.27)$$

Another possible configuration is the one with partially or completely restored chiral symmetry. Consider the phase where  $\sigma_1 = 0$ ,  $\sigma_2 \neq 0$ . For this configuration we need to use (2.10) with  $\partial_U X^4 = 0$  which corresponds to the limit  $U_0 \rightarrow 0$ ,  $\tilde{c} \rightarrow \infty$ . Hence, we can use some of the results above in the limit  $\tilde{c} \rightarrow \infty$ . The value of chemical potential is now

$$\mu_1 = c_1 c^{\frac{2}{5}} \quad (2.28)$$

which should be compared with (2.13) and (2.16). The value of  $\delta S$  is

$$\delta S_{1r} = E_0^{\frac{7}{2}} \left( G^7(0)H(0) + \frac{2}{7c_1^{\frac{5}{2}}} \tilde{\mu}^{\frac{7}{2}} \right) \quad (2.29)$$

Analogously, the value of the action for the phase with completely restored chiral symmetry is

$$\delta S_{12r} = E_0^{\frac{7}{2}} \frac{2}{7c_1^{\frac{5}{2}}} (\tilde{\mu}_1^{\frac{7}{2}} + \tilde{\mu}_2^{\frac{7}{2}}) \quad (2.30)$$

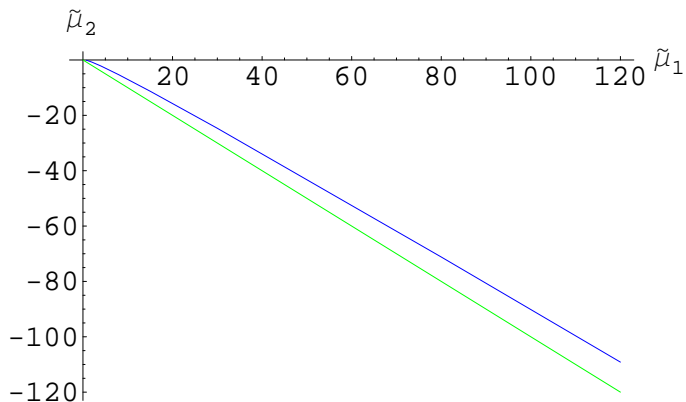


**Fig 2.** Phase diagram for  $LT \rightarrow 0$ .  $\mu_{1,2}$  are horizontal and vertical axes. Green line  $\tilde{\mu}_2 = -\tilde{\mu}_1$  is a boundary of the fundamental domain. Blue curve is the line of first order phase transitions between the phase with  $\rho \neq 0$  (below) and  $\rho = 0$  (above). The leading asymptotics is  $\mu_2 \approx -\mu_1$ .

Comparing (2.29), (2.30) and (2.27) we deduce the asymptotic behavior of the line of the phase transitions between the phase with  $\rho \neq 0$  and the phase with  $\rho = 0$ . This line (shown as a blue curve in Figs. 1,2) must behave asymptotically as  $\tilde{\mu}_2 \approx -\tilde{\mu}_1$  at large values of  $\tilde{\mu}_i$ .

More refined features of the phase diagram need numerical work. The results are summarized in Figs. 1,2. The green lines,  $\tilde{\mu}_2 = \pm\tilde{\mu}_1$  define the boundaries of the fundamental domain. For  $\tilde{\mu}_{1,2} > \tilde{\mu}_c$  the phase with straight branes dominates and all condensates vanish. Note that  $\tilde{\mu}_c$  is the value of  $\tilde{\mu}_B$  at the point of the phase transition in the  $\tilde{\mu}_I = 0$  plane. It is computed numerically to be  $\tilde{\mu}_c = 0.11$  at  $LT \rightarrow 0$ . For  $-\tilde{\mu}_c \leq \tilde{\mu}_2 \leq \tilde{\mu}_c$  but  $\tilde{\mu}_1$  to the right of the blue line, the phase with straight brane “1” but curved brane “2” (with vanishing electric field) dominates. This is the phase with  $\sigma_1 = 0$ ,  $\sigma_2 \neq 0$ . Below the blue line is the habitat of the curved solution with  $\rho \neq 0$ ,  $\sigma_1 = \sigma_2 = 0$ . Finally, all condensates vanish between the blue and the red lines, for sufficiently large values of  $\tilde{\mu}_B$  and  $\tilde{\mu}_I$ .

Fig. 2. depicts the phase diagram at a larger scale. As explained above, the blue phase transition line has the leading asymptotics  $\tilde{\mu}_2 \approx -\tilde{\mu}_1$ . The correction seems to behave like  $\sqrt{\tilde{\mu}_1}$ .

### 3. Intermediate temperatures

In this Section we consider the case of finite  $LT$ . As we will see, for sufficiently large values of  $LT$  the phases with nonzero condensates do not exist. We also assume that the temperature is sufficiently high, so that gluons are deconfined. This means that the black hole has formed in the holographic dual. The metric is now

$$ds^2 = \left(\frac{U}{R}\right)^{\frac{3}{2}} (f(U)dt^2 + \delta_{ij}dX^i dX^j + (dX^4)^2) + \left(\frac{U}{R}\right)^{-\frac{3}{2}} \left[\frac{(dU)^2}{f(U)} + U^2 d\Omega_4^2\right] \quad (3.1)$$

where

$$f(U) = 1 - \frac{U_T^3}{U^3}, \quad U_T = \frac{(4\pi)^2 \pi \lambda T^2}{9} \quad (3.2)$$

The dilaton is given by (2.5). The analysis of the previous Section corresponds to the  $U_T = 0$  limit. To determine the phase diagram in the  $\mu_1 - \mu_2$  plane at finite temperature we need to repeat the analysis of Section 2.

The DBI action now reads

$$S = 2 \int dU U^{\frac{5}{2}} \sqrt{1 - (\partial_U A_0)^2 + f(U) \left(\frac{U}{R}\right)^3 (\partial_U X^4)^2} \quad (3.3)$$

The analogs of (2.11) and (2.12) are

$$(\partial_U X^4)^2 = \frac{U_0^3 (U_0^5 + c^2) R^3 f(U_0)}{U^6 (U^5 + c^2) f^2(U) - U_0^3 (U_0^5 + c^2) U^3 f(U_0) f(U)} \quad (3.4)$$

and

$$(\partial_U A_0)^2 = \frac{c^2 U^3 f(U)}{U^3 (U^5 + U_0^5 \tilde{c}^2) f(U) - U_0^8 (1 + \tilde{c}^2) f(U_0)} \quad (3.5)$$

where we again used  $c^2 = U_0^5 \tilde{c}^2$ . It will be convenient to introduce dimensionless variables by rescaling

$$U_0 = u_0 E_0; \quad \mu_i = \tilde{\mu}_i E_0 \quad (3.6)$$

where  $E_0 = 4\pi\lambda/L^2$  as before.

Another useful quantity is

$$\tilde{t} = \frac{2\pi LT}{3} \quad (3.7)$$

Using equations of motion to compute  $L$  together with (3.6), and going to the rescaled variables, we obtain the following relation:

$$\tilde{t} = y^{\frac{1}{2}} G(\tilde{c}, y) \quad (3.8)$$

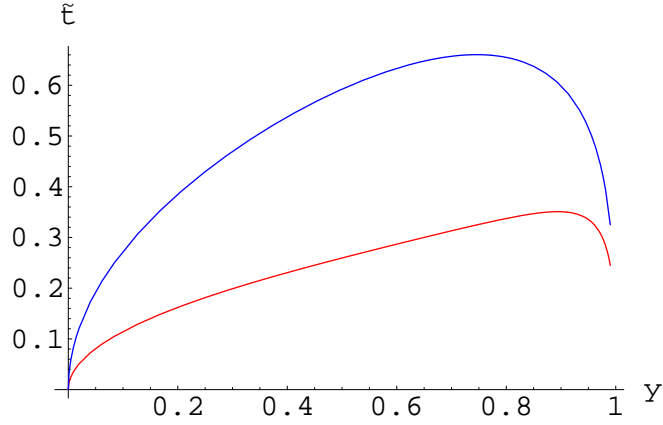


**Fig 3.**  $\tilde{t} = y^{\frac{1}{2}}G(\tilde{c}, y)$  [see eq. (3.8)] as a function of  $y$  at  $\tilde{c} = 0$  [red line] and  $\tilde{c} = 1 \times 10^6$  [blue line]. There is a limiting temperature beyond which the phase with connected branes does not exist.

where

$$y = \left(\frac{U_T}{U_0}\right)^3 = \frac{\tilde{t}^2}{u_0} \quad (3.9)$$

where we used (3.2), (3.6) and (3.7), and

$$G(\tilde{c}, y) = \int_1^\infty dx \sqrt{\frac{(1 + \tilde{c}^2)(1 - y^2)}{(x^5 + \tilde{c}^2)(x^3 - y^3)^2 - (1 + \tilde{c}^2)(x^3 - y^3)(1 - y^3)}} \quad (3.10)$$

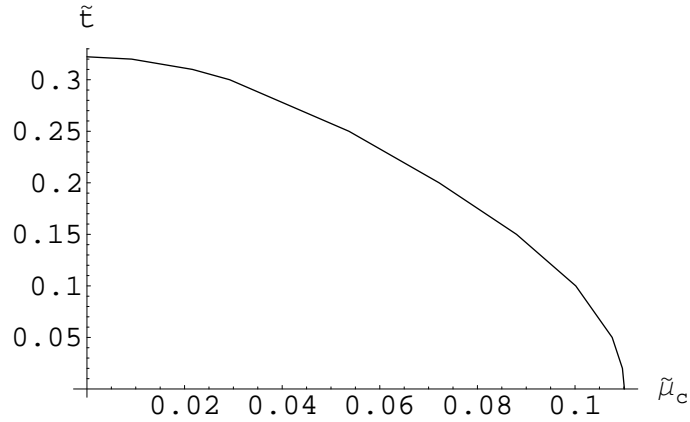


**Fig 4.** Phase transition line at  $\mu_I = 0$ . Horizontal axis is  $\tilde{\mu}_c$ . Vertical axis is  $\tilde{t}$ .

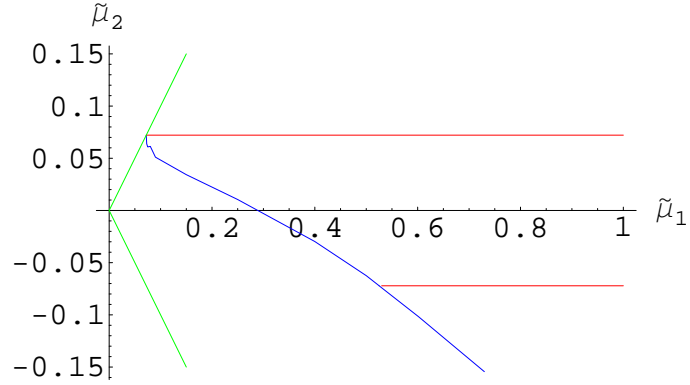


**Fig 5.** Phase diagram for  $\tilde{t} = 0.2$ .  $\mu_{1,2}$  are horizontal and vertical axes. Green lines  $\tilde{\mu}_2 = \pm\tilde{\mu}_1$  are boundaries of the fundamental domain. Solid blue and red curves are the lines of first order phase transitions. The phase between the red lines has  $\sigma_2 \neq 0$ . The phase between the blue and the green lines has  $\rho \neq 0$ . All other condensates vanish.

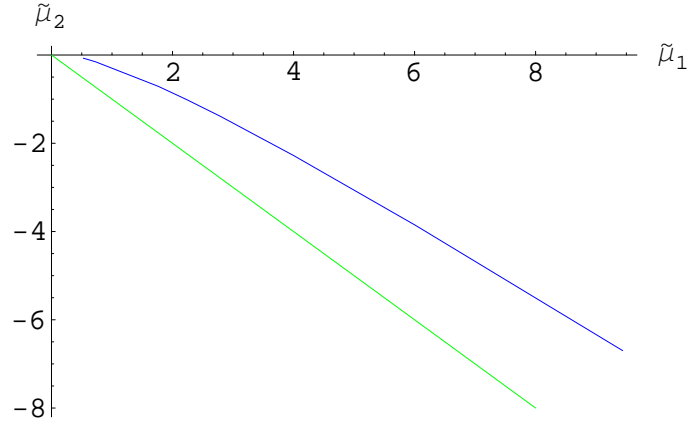


**Fig 6.** Phase diagram for  $\tilde{t} = 0.2$ .  $\mu_{1,2}$  are horizontal and vertical axes. Green line  $\tilde{\mu}_2 = -\tilde{\mu}_1$  is a boundary of the fundamental domain. Blue curve is the line of first order phase transitions between the phase with  $\rho \neq 0$  (below) and  $\rho = 0$  (above). The leading asymptotics is  $\mu_2 \approx -\mu_1$ .

At a given value of  $\tilde{t}$  (or, equivalently,  $LT$ ) (3.8) determines  $y$  (and  $u_0$ ) as a function of  $\tilde{c}$ . The behavior of the right hand side of (3.8) is shown in Fig. 3. There are two solutions of eq. (3.8). The one with larger  $y$  comes closer to the black hole horizon than its smaller  $y$

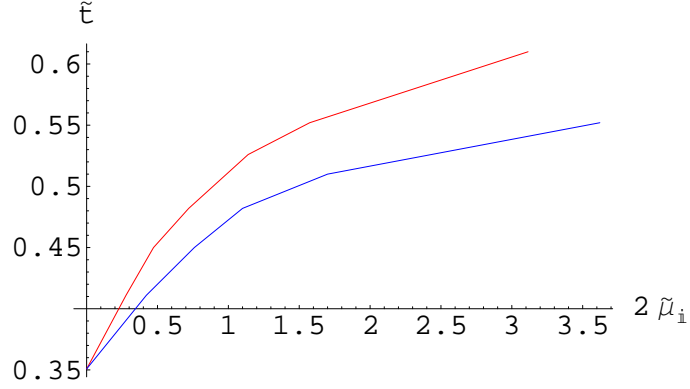


**Fig 7.** Line of phase transition [shown in blue; bottom line] in the  $\mu_B = 0$  plane. Horizontal axis is  $2\tilde{\mu}_I$ ; vertical axis is  $\tilde{t}$ . Red [top] line is the limiting value of  $\tilde{t}$ .

counterpart. It is the latter one which connects to the vacuum solution at  $T = 0$  and it is not hard to check that it is thermodynamically preferred. In the following we will focus on this solution. Note that for any value of  $\mu_I$  there is a limiting temperature beyond which the curved brane solution does not exist.

The next step is to compute  $\tilde{\mu}_I$

$$\frac{1}{2}|\tilde{\mu}_1 - \tilde{\mu}_2| = \frac{\tilde{t}^2}{y} F(\tilde{c}, y) \quad (3.11)$$

where

$$F(\tilde{c}, y) = \int_1^\infty dx \sqrt{\frac{\tilde{c}^2(x^3 - y^3)}{(x^5 + \tilde{c}^2)(x^3 - y^3) - (1 + \tilde{c}^2)(1 - y^3)}} \quad (3.12)$$

Using (3.8) and (3.11) one can determine  $\tilde{c}$  and  $y$  in terms of  $\tilde{\mu}_{1,2}$ . To determine the thermodynamically preferred state we need to compute the action in various phases. This is again done in a similar way as in the previous Section. The expression for  $\delta S$  with non-vanishing  $\rho$  is [compare with (2.22)]

$$\delta S = 2 \left[ \int_{U_T}^{U_0} dU U^{\frac{5}{2}} + \int_{U_0}^\infty dU U^{\frac{5}{2}} \left( 1 - \sqrt{\frac{U^8 f(U)}{U^3(U^5 + c^2)f(U) - U_0^3(U_0^5 + c^2)f(U_0)}} \right) \right] \quad (3.13)$$

In terms of rescaled variables, this becomes

$$\delta S = 2E_0^{\frac{7}{2}} \frac{\tilde{t}^7}{y^{\frac{7}{2}}} H(\tilde{c}, y) \quad (3.14)$$

where

$$H(\tilde{c}, y) = \frac{2}{7}(1 - y^{\frac{7}{2}}) + \int_1^\infty dx x^{\frac{5}{2}} \left( 1 - \sqrt{\frac{x^5(x^3 - y^3)}{(x^5 + \tilde{c}^2)(x^3 - y^3) - (1 + \tilde{c}^2)(1 - y^3)}} \right) \quad (3.15)$$

Note that the functions  $G(\tilde{c}, y)$ ,  $F(\tilde{c}, y)$ ,  $H(\tilde{c}, y)$  defined in (3.10), (3.12) and (3.15) respectively, reduce to the functions  $G(\tilde{c})$ ,  $F(\tilde{c})$ ,  $H(\tilde{c})$ , which were used in the previous Section, in the limit  $y \rightarrow 0$ .

The value of  $\delta S$  in the phase with curved branes and zero electric field ( $\sigma_1 = \sigma_2 \neq 0$ ,  $\rho = 0$ ) is

$$\delta S_0 = 2E_0^{\frac{7}{2}} \frac{\tilde{t}^7}{y^{\frac{7}{2}}} H(0, y) \quad (3.16)$$

where  $y$  is determined from (3.8) with  $\tilde{c} = 0$ . To analyze the phase diagram we also need to compute the value of the action in the phases with  $\sigma_i = 0$ ,  $\sigma_{j \neq i} \neq 0$  and  $\sigma_{1,2} = 0$ . The former is given by

$$\delta S_{ir} = \frac{\delta S_0}{2} + \int_{U_T}^\infty dU U^{\frac{5}{2}} \left( 1 - \sqrt{\frac{U^5}{U^5 + c^2}} \right) \quad (3.17)$$

where  $c$  is related to  $\mu_i$  as

$$\mu_i = \int_{U_T}^\infty dU \sqrt{\frac{c^2}{c^2 + U^5}} \quad (3.18)$$

In terms of the rescaled quantities,

$$\delta S_{ir} = \frac{\delta S_0}{2} + \frac{2}{7} E_0^{\frac{7}{2}} \tilde{t}^7 \left( \sqrt{1 + \frac{c^2}{\tilde{t}^{10}}} - 1 + \tilde{c}^{\frac{7}{5}} \frac{\Gamma(\frac{3}{10}) \Gamma(\frac{6}{5})}{\sqrt{5}} - \frac{\tilde{c}}{\tilde{t}^5} {}_2F_1 \left( \frac{1}{5}; \frac{1}{2}; \frac{6}{5}; -\frac{\tilde{t}^{10}}{\tilde{c}^2} \right) \right) \quad (3.19)$$

where  $\tilde{c}$  is determined through

$$\tilde{\mu}_i = \tilde{c}^{\frac{2}{5}} \int_{\frac{\tilde{t}^2}{\tilde{c}^{\frac{2}{5}}}}^\infty dx \sqrt{\frac{1}{x^5 + 1}} \quad (3.20)$$

Finally, the value of the  $\delta S$  for the phase with vanishing condensates is

$$\delta S_{12r} = \delta S_{1r} + \delta S_{2r} - 2\delta S_0 \quad (3.21)$$

We are ready to analyze the phase diagram. As explained at the end of Section 2,  $\tilde{\mu}_c(T)$  defines the line of phase transitions in the  $\tilde{\mu}_B, T$  plane at  $\tilde{\mu}_I = 0$ . Here we reproduce this plot for completeness in Fig. 4.

Figs. 5,6 contain the slice of the phase diagram in the  $\tilde{\mu}_1 - \tilde{\mu}_2$  plane for a sample value of  $\tilde{t} = 0.2$ . The pictures look similar to the ones in Figs. 1,2. The only visible difference is shrinking of the  $\tilde{\mu}_c$  with temperature, described by the curve in Fig. 4. Therefore the picture which emerges at large  $\tilde{\mu}_I$  is the surface of first order phase transitions in the  $\tilde{\mu}_B, \tilde{\mu}_I, T$  space whose sections are the blue lines in Figs. 2, 6. This surface resembles hyperboloid with  $\tilde{\mu}_I$  being the axis of rotation. To determine the behavior of the surface at large  $\tilde{\mu}_I$ , we consider  $\tilde{\mu}_B = 0$  plane.

In Fig. 7 we plot the curve which is obtained by intersecting the phase transition surface with the  $\tilde{\mu}_B = 0$  plane. Red line on this graph denotes the limiting value of  $\tilde{t}$ , beyond which the curved brane solution does not exist. Both lines seem to go to limiting values of  $\tilde{t}$  at large  $\mu_I$ . From this picture we see that the phase transition surface never intersects the limiting surface, and the transition remains first order.

#### 4. Conclusions

In this paper we analyzed the phase diagram of holographic QCD at finite temperature and baryon and isospin chemical potentials, defined by (2.2). The action (2.1) is invariant under  $\mu_1 \leftrightarrow \mu_2$ , which corresponds to  $\mu_I \rightarrow -\mu_I$ . Moreover, the physics is also invariant under  $\mu_i \rightarrow -\mu_i$ . Hence, the fundamental domain in the  $\mu_1, \mu_2$  plane can be taken to be (1.1). We found an intricate structure with various phases separated by the first order phase transitions.<sup>5</sup>

In particular, at large values of  $\mu_I$ , we found a surface of first order phase transitions which separates the phase with the nonzero value of  $\rho$  existing at smaller values of  $\mu_B$  from the chirally restored phase at larger values of  $\mu_B$ .

It is not hard to reinstate gluon confinement/deconfinement transition in the phase diagram. It is represented as a surface  $T = 1/2\pi R_4$ . For temperatures lower than this value chiral symmetry is necessarily broken and the system is in the phase with nonzero electric flux on the branes. We do not analyze this phase in detail here. It is clear that in the regions of the phase space where chiral symmetry is broken, the surface  $T = 1/2\pi R_4$  describes the coincident confinement/deconfinement and chiral phase transitions.

---

<sup>5</sup> As usual in the DBI analysis, the free energies of different phases have different values of the derivatives at the crossing point, indicating first order phase transitions.



An important observation concerns the energy scales in the problem. We have seen that the relevant variables in the phase space are  $LT$  and  $\mu/E_0$ . This is consistent with the energy scales of the mesons being  $\mathcal{O}(1/L)$  and constituent masses of quarks being  $\mathcal{O}(E_0)$ .

The DBI action used to analyze the structure of the phase diagram in this paper is essentially abelian. It would be interesting to investigate the effect of non-abelian degrees of freedom, in particular with regards to the stability of the solutions. The existence of other phases also cannot be ruled out. Other directions for future research include generalizing our results to a higher number of flavors and studying other holographic models of QCD-like theories.

## 5. Acknowledgments

I would like to thank R. Casalbuoni, T. Schaefer and J. Verbaarschot for useful discussions. I also thank the organizers of the “Exploring QCD: Deconfinement, Extreme Environments and Holography” workshop at Newton Institute, Cambridge, for stimulating environment.

## References

- [1] T. Sakai and S. Sugimoto, “Low energy hadron physics in holographic QCD,” *Prog. Theor. Phys.* **113**, 843 (2005) [arXiv:hep-th/0412141].
- [2] E. Witten, “Anti-de Sitter space, thermal phase transition, and confinement in gauge theories,” *Adv. Theor. Math. Phys.* **2**, 505 (1998) [arXiv:hep-th/9803131].
- [3] O. Aharony, J. Sonnenschein and S. Yankielowicz, “A holographic model of deconfinement and chiral symmetry restoration,” *Annals Phys.* **322**, 1420 (2007) [arXiv:hep-th/0604161].
- [4] A. Parnachev and D. A. Sahakyan, “Chiral phase transition from string theory,” *Phys. Rev. Lett.* **97**, 111601 (2006) [arXiv:hep-th/0604173].
- [5] N. Horigome and Y. Tanii, “Holographic chiral phase transition with chemical potential,” *JHEP* **0701**, 072 (2007) [arXiv:hep-th/0608198].
- [6] A. Parnachev and D. A. Sahakyan, “Photoemission with chemical potential from QCD gravity dual,” *Nucl. Phys. B* **768**, 177 (2007) [arXiv:hep-th/0610247].
- [7] K. Y. Kim, S. J. Sin and I. Zahed, “Dense hadronic matter in holographic QCD,” arXiv:hep-th/0608046.
- [8] K. Y. Kim, S. J. Sin and I. Zahed, “The Chiral Model of Sakai-Sugimoto at Finite Baryon Density,” arXiv:0708.1469 [hep-th].
- [9] O. Bergman, G. Lifschytz and M. Lippert, “Holographic Nuclear Physics,” arXiv:0708.0326 [hep-th].
- [10] J. L. Davis, M. Gutperle, P. Kraus and I. Sachs, “Stringy NJL and Gross-Neveu models at finite density and temperature,” arXiv:0708.0589 [hep-th].
- [11] M. Rozali, H. H. Shieh, M. Van Raamsdonk and J. Wu, “Cold Nuclear Matter In Holographic QCD,” arXiv:0708.1322 [hep-th].
- [12] J. Erdmenger, M. Kaminski and F. Rust, “Isospin diffusion in thermal AdS/CFT with flavor,” *Phys. Rev. D* **76**, 046001 (2007) [arXiv:0704.1290 [hep-th]].
- [13] D. T. Son and M. A. Stephanov, “QCD at finite isospin density,” *Phys. Rev. Lett.* **86**, 592 (2001) [arXiv:hep-ph/0005225].
- [14] B. Klein, D. Toublan and J. J. M. Verbaarschot, “The QCD phase diagram at nonzero temperature, baryon and isospin chemical potentials in random matrix theory,” *Phys. Rev. D* **68**, 014009 (2003) [arXiv:hep-ph/0301143].
- [15] D. Toublan and J. B. Kogut, “Isospin chemical potential and the QCD phase diagram at nonzero temperature and baryon chemical potential,” *Phys. Lett. B* **564**, 212 (2003) [arXiv:hep-ph/0301183].
- [16] A. Barducci, R. Casalbuoni, G. Pettini and L. Ravagli, “A calculation of the QCD phase diagram at finite temperature, and baryon and isospin chemical potentials,” *Phys. Rev. D* **69**, 096004 (2004) [arXiv:hep-ph/0402104].

- [17] E. Antonyan, J. A. Harvey, S. Jensen and D. Kutasov, “NJL and QCD from string theory,” arXiv:hep-th/0604017.
- [18] E. Antonyan, J. A. Harvey and D. Kutasov, “The Gross-Neveu model from string theory,” Nucl. Phys. B **776**, 93 (2007) [arXiv:hep-th/0608149].
- [19] E. Antonyan, J. A. Harvey and D. Kutasov, “Chiral symmetry breaking from intersecting D-branes,” Nucl. Phys. Proc. Suppl. **171**, 243 (2007) [arXiv:hep-th/0608177].